Electronic Supplementary Material (ESI) for RSC Advances.

Supporting Information

Large enhanced photocatalytic activity of g-C_3N_4 by fabrication of a nanocomposite with introducing upconversion nanocrystal and Ag nanoparticles

Feifei Zhao, Kyu Kyu Khaing, Dongguang Yin*, Bingji Liu, Tao Chen, Chenglong Wu, Kexian Huang, LinLin Deng, Luqiu Li

School of Environmental and Chemical Engineering, Shanghai University, Shanghai, 200444, E-mail: ydg@shu.edu.cn

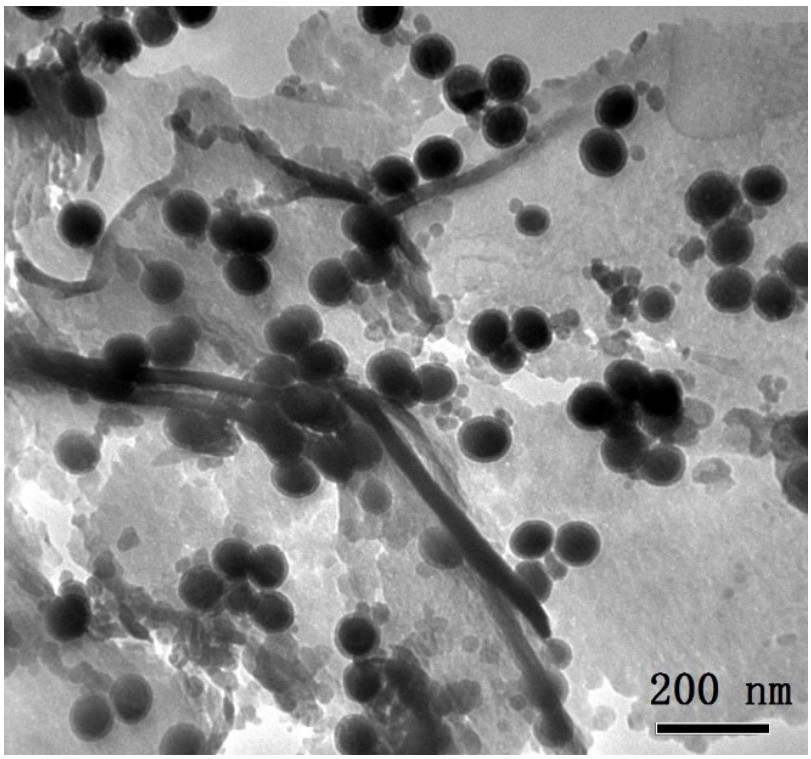

Fig. S1. TEM image of UCNPs@SiO_2/g-C_3N_4.

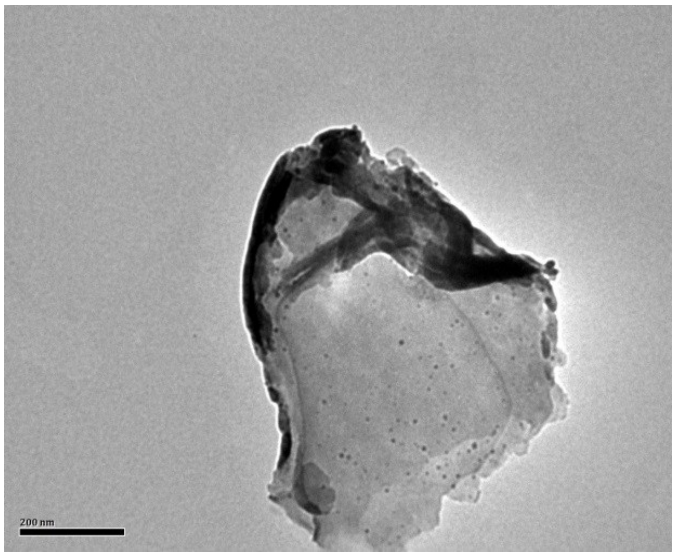

Fig. S2. TEM image of 3wt%Ag/g-C_3N_4.

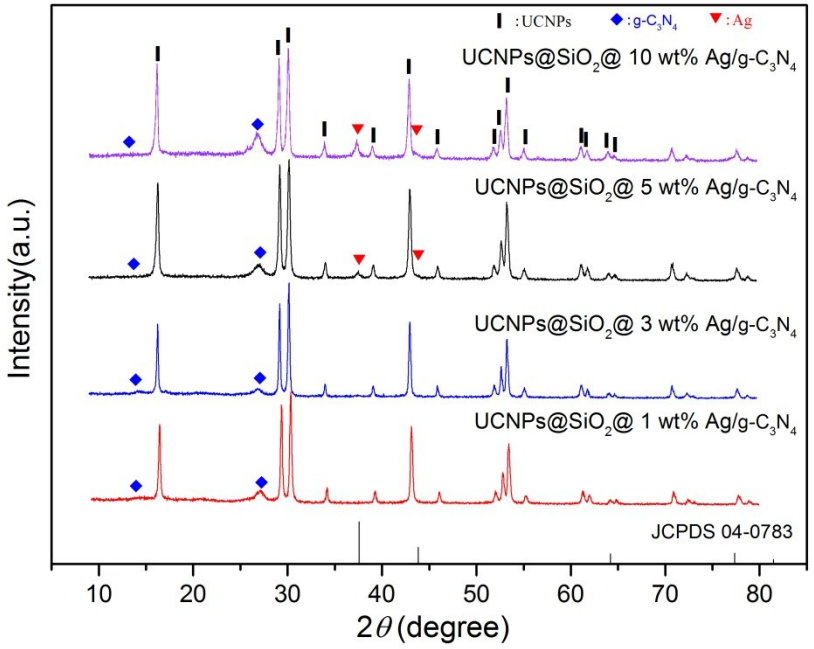

Fig. S3. XRD patterns of the UCNPs@SiO_2@*X*wt% Ag/g-C_3N_4 nanocomposites with different doping amounts of Ag (*X* =1, 3, 5, and 10). The corresponding standard data for the face-centered cubic phase of silver (JCDS 04-0783) is also given at the bottom.

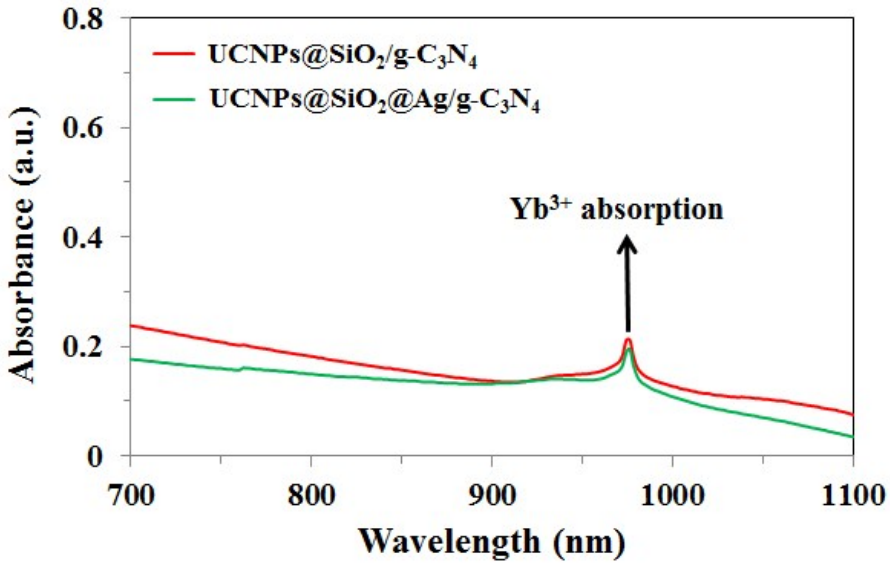

Fig. S4. Absorption spectra of UCNPs@SiO_2/g-C_3N_4 and UCNPs@SiO_2@Ag/g-C_3N_4 nanocomposites in ethanol.

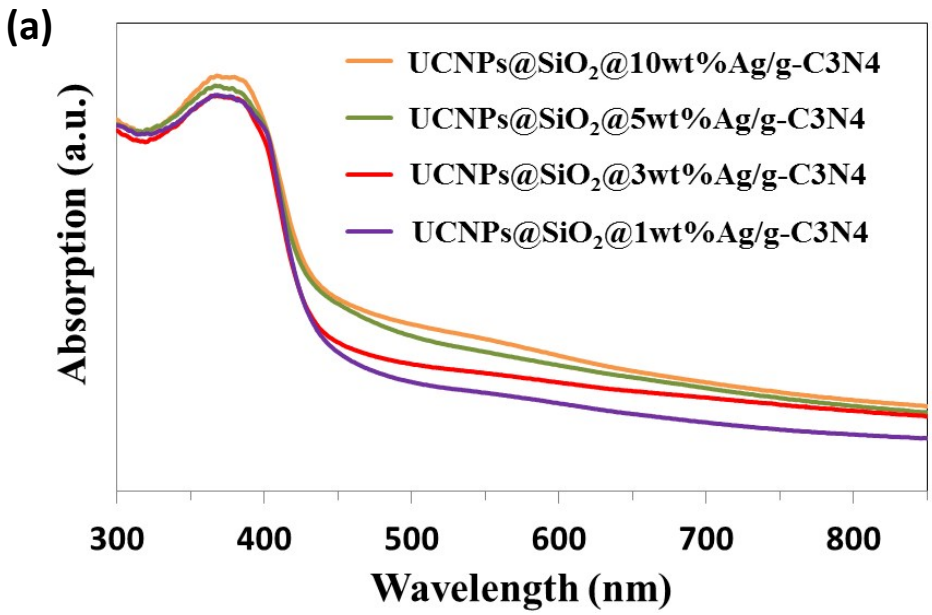

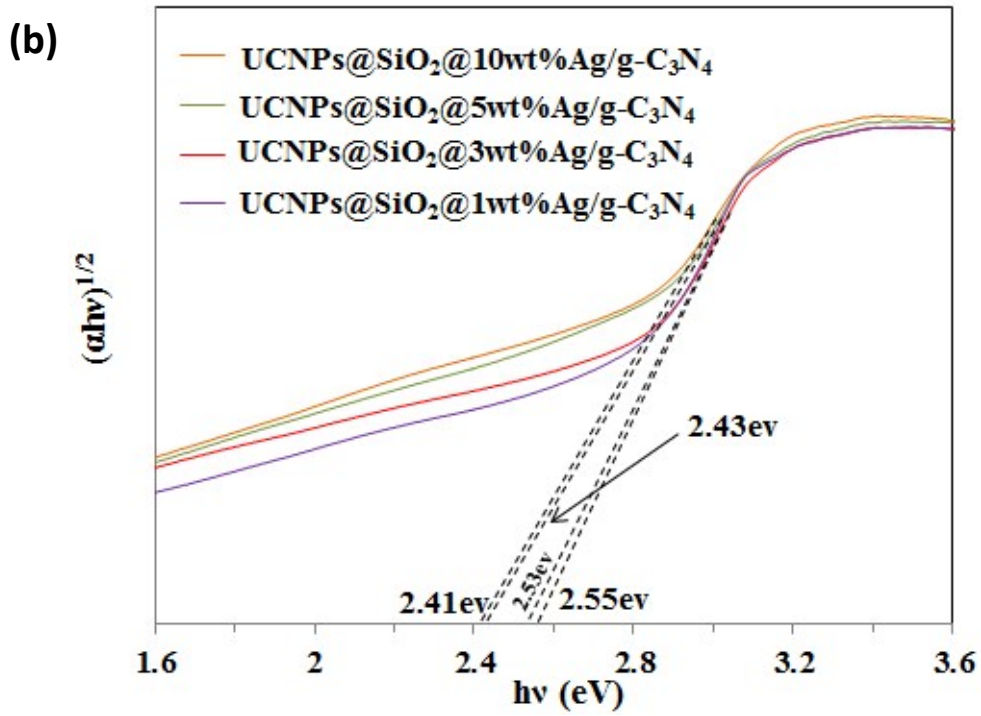

Fig. S5. (a) UV-Vis-NIR diffuse reflectance spectra of UCNPs@SiO_2@Xwt% Ag/g-C3N4 nanocomposites with different doping amounts of Ag (X =1, 3, 5, and 10). (b) Plots of $(\alpha h\nu)^{1/2}$ vs. photon energy ($h\nu$).

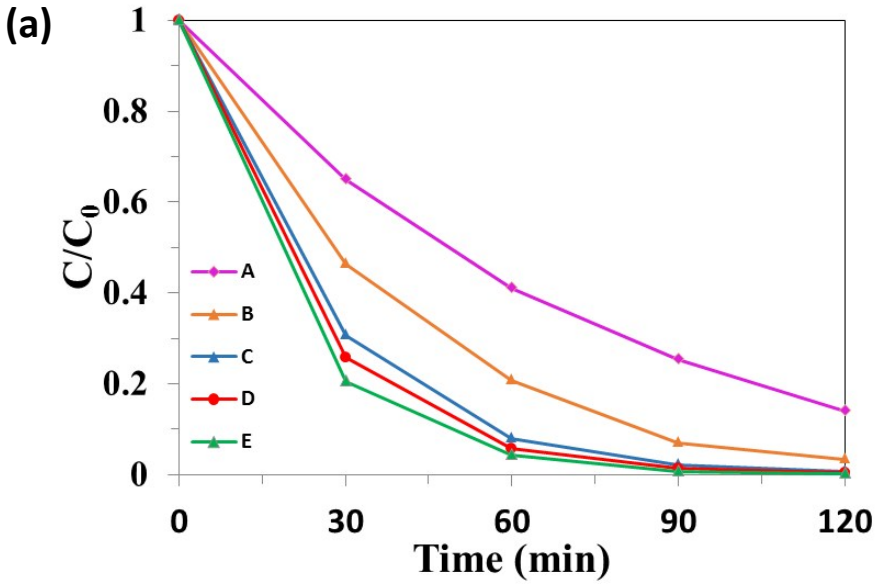

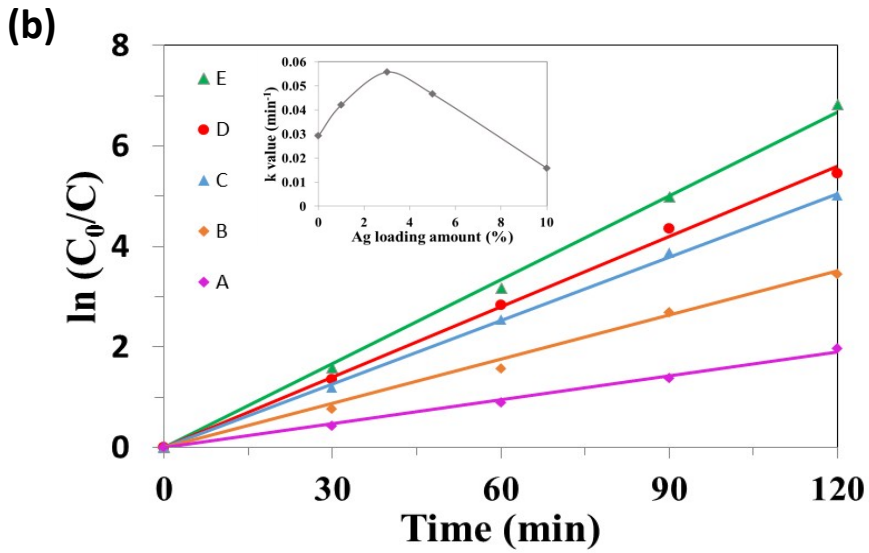

Fig. S6. (a) Photocatalytic degradation of RhB and (b) the kinetics study over different photocatalysts under simulated solar light irradiation: (A) UCNPs@SiO_2@10wt%Ag/g-C_3N_4; (B) UCNPs@SiO_2/g-C_3N_4; (C) UCNPs@SiO_2@1wt%Ag/g-C_3N_4; (D) UCNPs@SiO_2@5wt%Ag/g-C_3N_4; (E) UCNPs@SiO_2@3wt%Ag/g-C_3N_4. The inset in (b) shows the rate constants vs Ag loading.

The possible mechanism of photocatalytic degradation of RhB in the present of UCNPs@SiO_2@Ag/g-C_3N_4 photocatalyst under simulated solar light irradiation is depicted in Fig. S7. After absorbing the solar and upconverted light, the excited g-C_3N_4 generates electron-hole pairs. The electrons transfer from the VB of g-C_3N_4 to the surface of Ag NPs. These electrons accumulated on the surface of Ag NPs react with O_2 to produce $\bullet O_2^-$ radicals, while the holes in the VB of g-C_3N_4 can react with OH^-/H_2O to generate •OH radicals. These reactive radicals and holes can directly take part in the photocatalytic degradation reaction to degrade RhB.

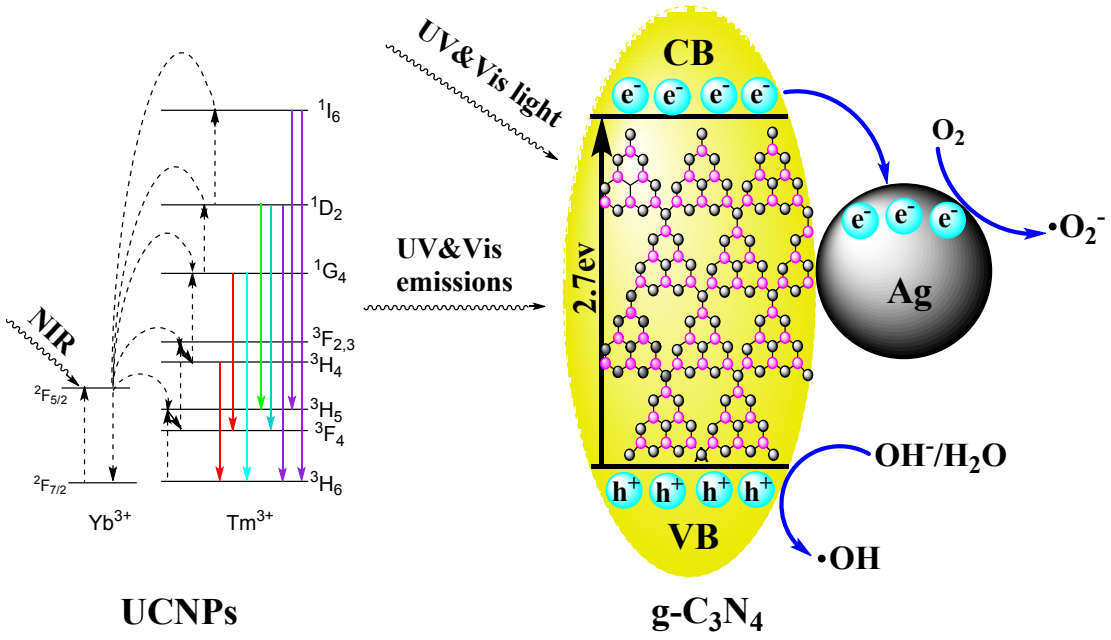

Fig. S7. Schematic illustration of photocatalytic mechanism of degradation of RhB over UCNPs@SiO_2@Ag/g-C_3N_4 photocatalysts under simulated solar light irradiation.

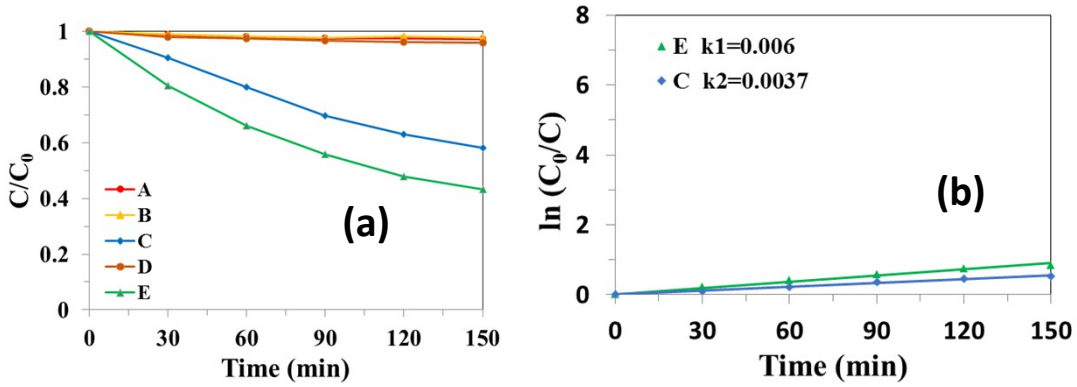

Fig. S8. (a) Photocatalytic degradation of RhB and (b) the kinetics study over different photocatalysts under NIR light irradiation: (A) UCNPs@SiO_2@Ag; (B) bulk g-C_3N_4; (C) UCNPs@SiO_2/g-C_3N_4; (D) Ag/g-C_3N_4; (E) UCNPs@SiO_2@3wt%Ag/g-C_3N_4.

The XPS spectra of the as-synthesized UCNPs@SiO_2@3wt%Ag/g-C_3N_4 nanocomposite were analyzed to further confirm the chemical composition and the

status of the elements. The XPS spectra of UCNPs@SiO_2@3wt%Ag/g-C_3N_4 are shown in Fig. S9. The C 1s spectrum has four distinct peaks centered at 284.12, 285.30, 287.51 and 292.22 eV, which are assigned to the adventitious carbon (C–C), the sp^3-hybridized carbon (C–$(N)_3$), the sp^2-hybridized carbon (N–C=N) and π–π*. The N 1s spectrum is separated into four peaks centered at 398.12, 398.96, 400.66 and 404.00 eV, which are assigned to the sp^2-hybridized nitrogen in aromatic triazine rings (C–C=N), the tertiary nitrogen (N-$(C)_3$), the free amino groups (C–N–H), and the charging effects or positive charge localization in the heterocycles, respectively. The Ag 3d spectrum presents two individual peaks at about 367.60 and 373.60 eV with 6.0 eV splitting between the two peaks, which corresponds to the metallic Ag^0 species. The binding energies at 102.50 eV and 531.97 eV are attributed to the Si^{4+} and O^{2-}, respectively, suggesting the existence of SiO_2. XPS peaks of Na (1s, 1072.47 eV), Gd (4d, 140.46 eV), F (1s, 685.85 eV), Lu ($4d_{5/2}$, 197.11 eV), Lu ($4d_{3/2}$, 206.53 eV), Yb (4d, 182.37 eV), and Tm (4d, 175.39 eV) are also found in Fig. S9 f~k.

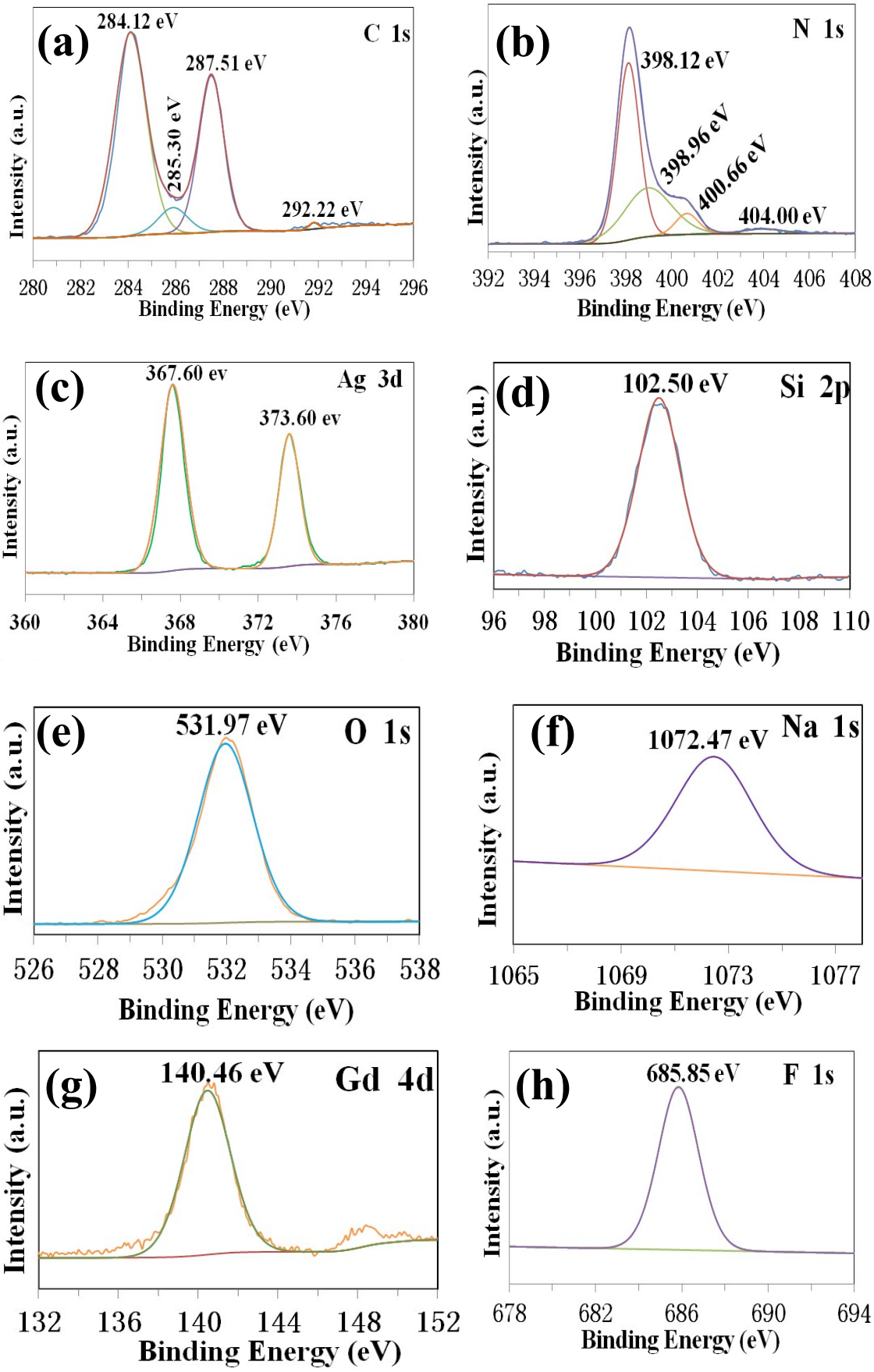
(a)
284.12 eV
287.51 eV
285.30 eV
292.22 eV
C 1s
Intensity (a.u.)
280 282 284 286 288 290 292 294 296
Binding Energy (eV)
(b)
398.12 eV
398.96 eV
400.66 eV
404.00 eV
N 1s
Intensity (a.u.)
392 394 396 398 400 402 404 406 408
Binding Energy (eV)
(c)
367.60 ev
373.60 ev
Ag 3d
Intensity (a.u.)
360 364 368 372 376 380
Binding Energy (eV)
(d)
102.50 eV
Si 2p
Intensity (a.u.)
96 98 100 102 104 106 108 110
Binding Energy (eV)
(e)
531.97 eV
O 1s
Intensity (a.u.)
526 528 530 532 534 536 538
Binding Energy (eV)
(f)
1072.47 eV
Na 1s
Intensity (a.u.)
1065 1069 1073 1077
Binding Energy (eV)
(g)
140.46 eV
Gd 4d
Intensity (a.u.)
132 136 140 144 148 152
Binding Energy (eV)
(h)
685.85 eV
F 1s
Intensity (a.u.)
678 682 686 690 694
Binding Energy (eV)

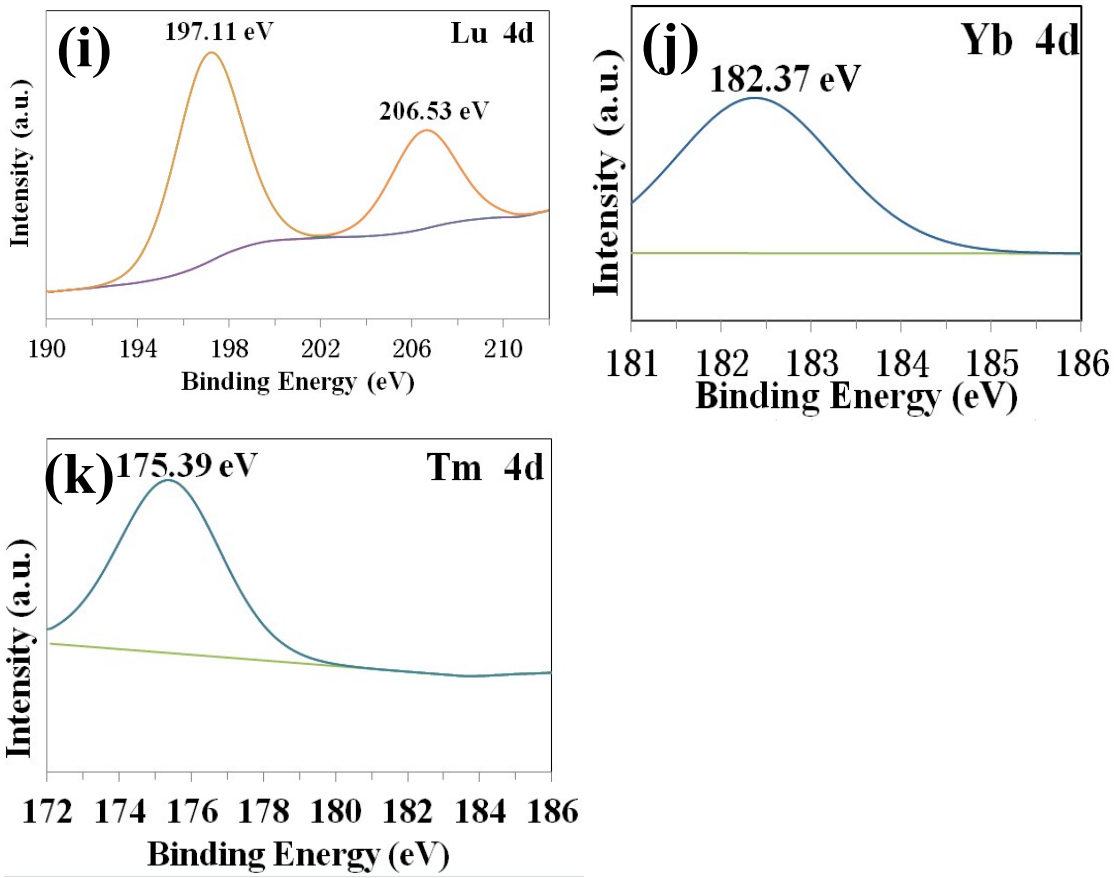

Fig. S9. XPS spectra of UCNPs@SiO_2@3wt%Ag/g-C_3N_4 nanocomposite: (a) C 1s, (b) N 1s, (c) Ag 3d, (d) Si 2p, (e) O 1s, (f) Na 1s, (g) Gd 4d, (h) F 1s, (i) Lu 4d, (j) Yb 4d, (k) Tm 4d.

Table. S1. Comparison with different photocatalysts for photocatalytic degradation of organic pollutant under simulated solar light irradiation.

photocatalyst	organic pollutant	time (min)	efficiency	reference
g-C_3N_4	RhB	150	62%	this work
UCNPs@SiO_2/g-C_3N_4	RhB	150	100%	this work
Ag/g-C_3N_4	RhB	120	100%	this work
UCNPs@SiO_2@1wt%Ag/g-C_3N_4	RhB	90	98%	this work
UCNPs@SiO_2@3wt%Ag/g-C_3N_4	RhB	90	100%	this work
UCNPs@SiO_2@5wt%Ag/g-C_3N_4	RhB	90	99%	this work

UCNPs@SiO_2@10wt%Ag/g-C_3N_4	RhB	90	75	this work
$NaYF_4$:Yb^{3+},Er^{3+},Tm^{3+}/g-C_3N_4	methyl orange	420	47%	23
Au-$NaYF_4$:Yb^{3+},Er^{3+},Tm^{3+}/g-C_3N_4	methyl orange	420	83%	23
UCNPs@SiO_2/TiO_2	RhB	210	83.98%	25
UCNPs@SiO_2@Ag/TiO_2	RhB	210	99.46%	25
UCNPs@SiO_2@CeO_2	RhB	210	63%	26
UCNPs@SiO_2@CeO_2:Tm	RhB	210	82%	26
UCNPs@SiO_2@CeO_2:Tm/GN	RhB	210	95%	26

Table. S2. Comparison with different photocatalysts for photocatalytic hydrogen evolution.

photocatalyst	sacrificial agent	H_2 generation rate ($\mu mol \cdot h^{-1} \cdot g^{-1}$)	light (nm)	reference
g-C_3N_4	triethanolamine	72	190-1100	this work
UCNPs@SiO_2/g-C_3N_4	triethanolamine	319	190-1100	this work
Ag/g-C_3N_4	triethanolamine	507	190-1100	this work
UCNPs@SiO_2@Ag/g-C_3N_4	triethanolamine	873	190-1100	this work
Pr^{3+}-Y_2SiO_5/$CaTiO_3$	perfluorodecalin	1.05	420-1100	57
$SrTiO_3$-Er^{3+}	Na_2SO_3/Na_2S	46.23	420-1100	58